Pumping Between Phases With a Pulsed-Fuel Molecular Ratchet

Dean Thomas,[1] Daniel J. Tetlow,[1] Yansong Ren,[1] Salma Kassem,[1] Ulvi Karaca,[1] and David A. Leigh*[1,2]

[1]Department of Chemistry, University of Manchester, Oxford Road, Manchester M13 9PL, UK

[2]School of Chemistry and Molecular Engineering, East China Normal University, 200062 Shanghai, China

*Correspondence to: david.leigh@manchester.ac.uk

The sorption of species from solution into and onto solids, surfaces, crystals, gels and other matrices, underpins the sequestering of waste and pollutants, the recovery of precious metals, heterogeneous catalysis, many forms of chemical and biological analysis and separation science, and numerous other technologies.[1-3] In such cases the transfer of the substrate between phases tends to proceed spontaneously, in the direction of equilibrium. Molecular ratchet mechanisms,[4-7] where kinetic gating[8-12] selectively inhibits or accelerates particular steps in a process, makes it possible to drive dynamic systems[13-16] out of equilibrium[17-22]. Here we report on a small-molecule pump[23] immobilised on and near the surface[24-26] of polymer beads, that uses an energy ratchet mechanism[18-22,27-31] to actively transport substrates from solution onto the beads away from equilibrium. One complete cycle of the pump occurs with each pulse of a chemical fuel,[20,32-36] synchronizing the ratchet dynamics so that the immobilised molecular machines all act in unison. Upon addition of the trichloroacetic acid (CCl_3CO_2H) fuel,[20,35,37,38] micrometre-diameter polystyrene beads functionalised with an average of ~8×10^{10} molecular pumps per bead,[39] sequester from solution crown ethers appended with a fluorescent tag (Fig. 1). Following consumption of the fuel, the rings are mechanically trapped in a higher energy, out-of-equilibrium, state on the beads and cannot be removed by dilution nor by switching the binding interactions off. This differs from dissipative assembled materials that require a continuous supply of energy to persist.[13-16] Addition of a second pulse of fuel causes the uptake of more macrocycles, which can be labelled with a different fluorescent tag. This drives the system progressively further away from equilibrium and also confers sequence information[40] on the deposited structure. The polymer-bound substrates (and the stored energy) can subsequently be released back to the bulk on demand,[41-43] either emptying one compartment at a time or all at once. Non-equilibrium[44] sorption by using immobilised artificial molecular machines[45-51] to pump substrates from solution onto and into

materials[52], offers potential[53,54] for the transduction of energy from chemical fuels for the storage and release of energy and information.

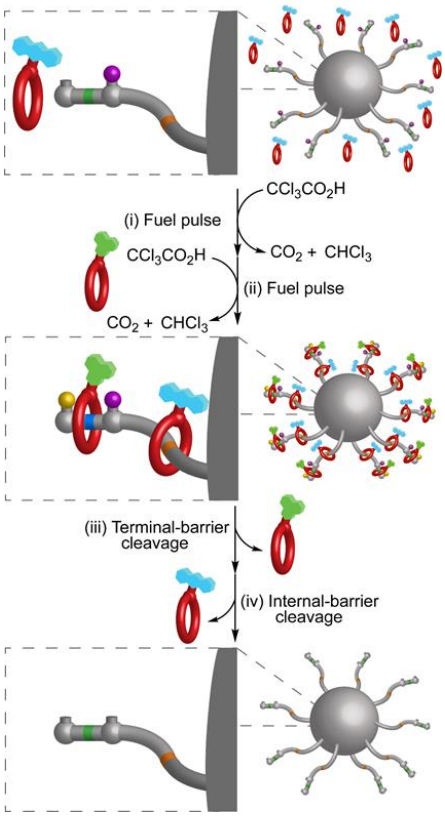

Fig. 1 | Pumping from solution to the solvent-accessible sites of polymer beads with a pulsed chemical fuel. (i and ii) Progressive pumping away from equilibrium of fluorophore-labelled macrocycles from acetonitrile solution onto polystyrene beads using a molecular ratchet and pulses of a chemical fuel (CCl_3CO_2H), followed by (iii and iv) sequential release of the bound substrates.

Building on theory,[27] the demonstration that energy[28,29] and information[17,55] ratchet mechanisms[4,10] can drive molecular systems away from equilibrium enabled the design of molecular motors[28,55] and pumps[17,29]. The molecular ratchet used in the present study is modified from a design[20] that drives small-molecule rotary motors or pumps in response to variations in pH, achieved either by sequential additions of acid and base or by discrete pulses of a single chemical fuel. In the new design the crown ether is reduced in size from dibenzo-30-crown-10 (DB30C10) to dibenzo-24-crown-8 (DB24C8), which model studies found substantially increased the threading efficacy of the pump. This requires a concomitant reduction in the thickness of the track the ring has to pass over when the internal and external barriers are open, leading to molecular ratchet design **1** (Fig. 2).

Under acidic conditions, DB24C8 can thread onto the axle of **1**, passing the dynamically labile hydrazone barrier to bind to a dibenzylammonium unit. Raising the pH then simultaneously kinetically locks the hydrazone barrier in place, preventing dethreading, and deprotonates the dibenzylammonium group to form a weakly binding amine, raising the macrocycle to a high energy state on the axle (Fig. 2b). Under the basic conditions the disulfide barrier can

exchange with free thiol in bulk solution. The macrocycle can therefore shuttle past the dynamically labile disulfide barrier to the triazolium site, which is a stronger binding site for the ring than the amine.[56] Switching back to acidic conditions then locks the disulfide barrier in place, trapping the crown ether in the triazolium compartment, whilst simultaneously triggering hydrazone exchange again. This causes a second macrocycle to be threaded from solution onto the reformed dibenzylammonium site, whilst retaining the first macrocycle that is locked in the compartment containing the triazolium group.

In order to isolate and characterise the individual steps of the pumping cycle, we first examined the operation of pump **1** in solution *via* the stepwise addition of acid and base (Fig. 2). Combining **1** and DB24C8 in CD_3CN at room temperature results in no detectable change to the ^1H NMR resonances of either component, confirming that threading does not occur under neutral conditions. Addition of trifluoroacetic acid (CF_3CO_2H) and hydrazide **2** resulted in the rapid appearance of the hydrazone peak H_e of capped [2]rotaxane **3**H^+ at 8.4 ppm. Quantitative threading onto the axle occurred over the period of one hour, evidenced by a downfield shift of H_h and H_i by ~1.0 ppm and an upfield shift of H_f and H_k by ~0.2 ppm (Fig. 3c). Formation of **3**H^+ was confirmed by electrospray ionisation-mass spectrometry (ESI-MS; see Supplementary Information, Section 2.1).

Subsequent addition of 1,8-diazabicyclo(5.4.0)undec-7-ene (DBU) deprotonated the dibenzylammonium group of **3**H^+, affording [2]rotaxane **3**. Addition of thiol **4** and disulfide **5** resulted in shuttling of the macrocycle past the now-dynamically-labile disulfide barrier to the triazolium group, forming [2]rotaxane **6** (Fig. 3d). The position of the macrocycle in **6** causes the ^1H NMR resonances of H_f, H_h, H_i and H_k to return to similar chemical shift values to those in **1**, and the broadening of H_o and H_m. Under these conditions the threading-shuttling cycle took ~16 hours to complete. Repeating the addition of CF_3CO_2H then generated [3]rotaxane **7**H^+ (Fig. 3e and Supplementary Information, Section 2.1), an out-of-equilibrium concentration of rings on the axle that is only possible through **1** acting as a molecular ratchet. Finally, a second addition of DBU to **7**H^+ deprotonated the dibenzylammonium group, the barriers trapping both macrocycles of **7** in high-energy states on the axle (Fig. 2b, bottom potential energy diagram).

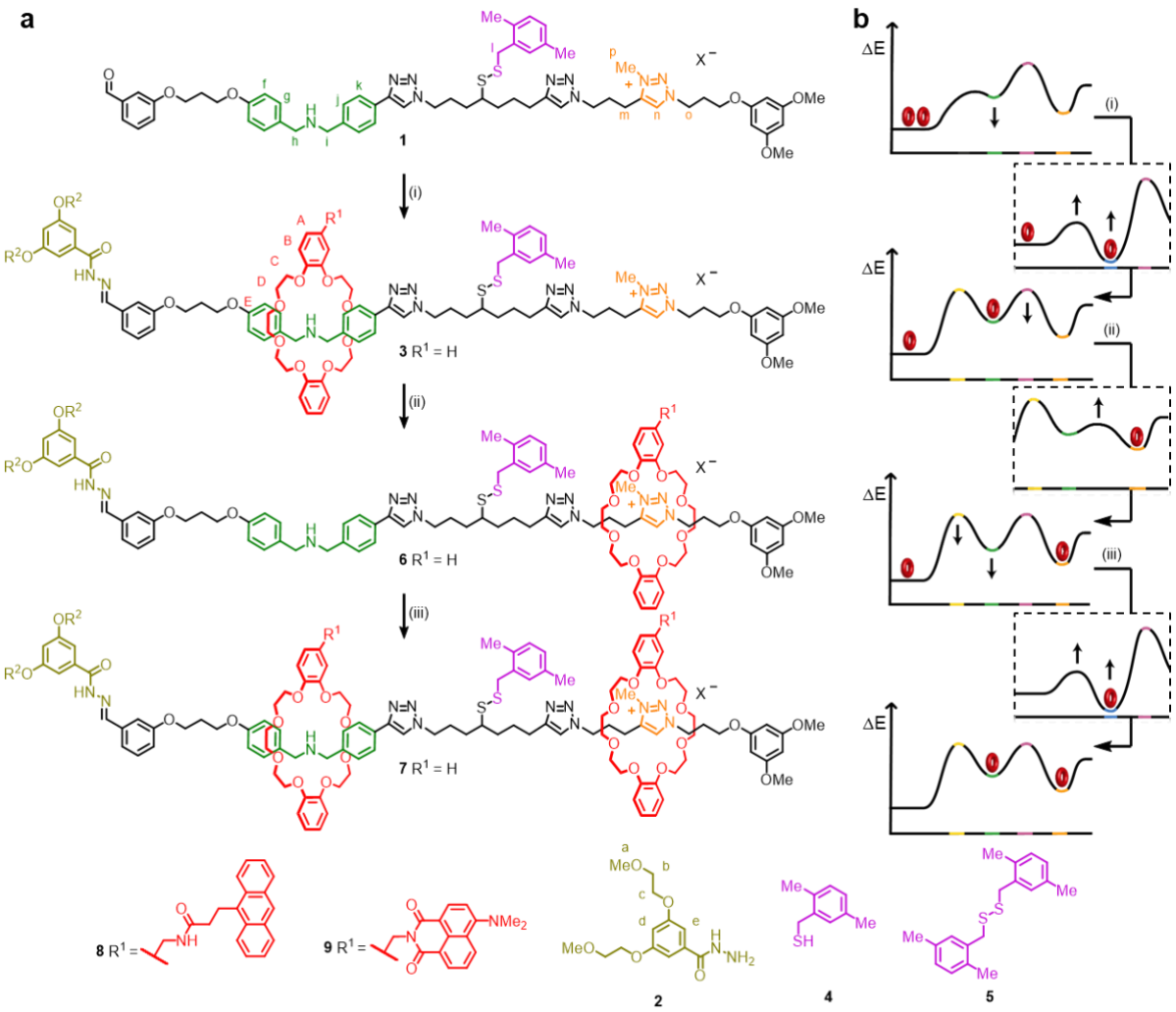

Fig. 2 | Stepwise operation of molecular pump 1 in solution. **a**, Reagents & conditions: (i) Pump **1** (9 mM, 1.0 equiv.), DB24C8 (3.0 equiv.), hydrazide **2** (1.2 equiv.), CF_3CO_2H (6.0 equiv.), CD_3CN, r.t., 1 h, then DBU (11 eq.), 65%. (ii) [2]rotaxane **3** (6 mM, 1.0 equiv.), thiol **4** (1.2 equiv.), disulfide **5** (12 equiv.), DBU (10 equiv.), CD_3CN, r.t., 16 h, 80%. (iii) [2]rotaxane **6** (5 mM, 1.0 equiv.), DB24C8 (4.0 equiv.), hydrazide **2** (1.3 equiv.), CF_3CO_2H (6.0 equiv.), CD_3CN, r.t., 4 h, then DBU (16 eq.), 63%. X^- denotes different anions that change during the operation, see Supplementary Information, Section 2. Yields were determined following isolation by size-exclusion chromatography. **b**, Illustrative potential energy diagrams of the machine operation, showing pumping away from equilibrium to the high energy state of the substrate.

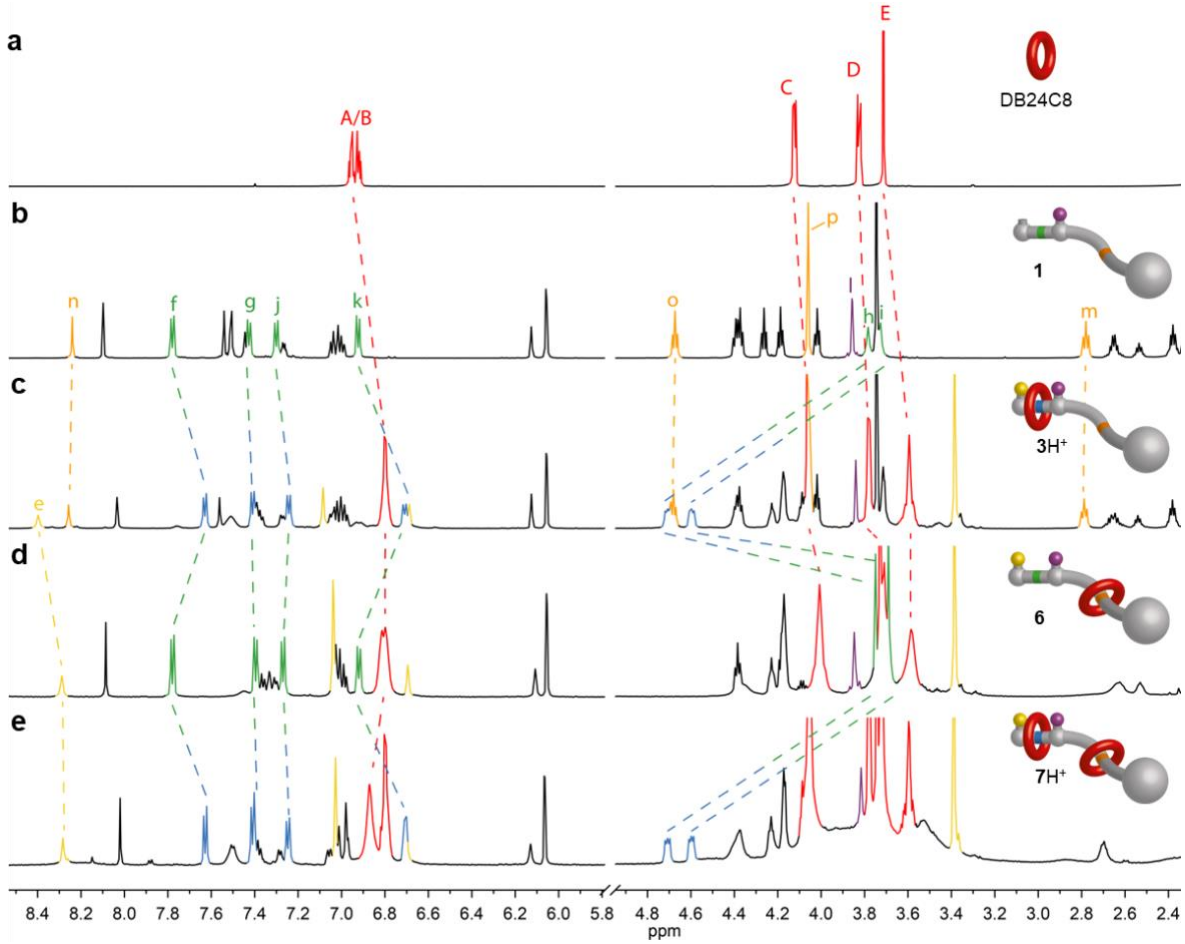

Fig. 3 | Partial ^{1}H NMR (600 MHz, CD_3CN, 298 K) spectra for the operation of molecular ratchet 1 in solution. **a**, DB24C8. **b**, Molecular ratchet **1**. **c**, [2]rotaxane **3**H$^+$, isolated after reaction of **1** with CF_3CO_2H, DB24C8 and hydrazide **2**. **d**, [2]rotaxane **6**, isolated after reaction of **3**H$^+$ with DBU, thiol **4** and disulfide **5**. **e**, [3]rotaxane **7**H$^+$, isolated after reaction of **6** with CF_3CO_2H, DB24C8 and hydrazide **2**. Lettering relates protons in the chemical structures shown in Fig. 2a to the corresponding signals in the ^{1}H NMR spectra.

Having used the sequential operation of **1** to isolate and characterise each intermediate in the mechanism of the ratchet, we next operated **1** with a single chemical fuel, trichloroacetic acid (CCl_3CO_2H), which decarboxylates in the presence of a catalytic base to generate chloroform and carbon dioxide as waste products.[20,35,37,38] A pulse of CCl_3CO_2H provides transient acidic conditions for a period of time that can be tuned, removing the need for stepwise addition of acid and base as basic conditions are restored upon full decarboxylation of the fuel[20]. Pleasingly, addition of a pulse of CCl_3CO_2H to a mixture of **1**, DB24C8, **2**, **4**, **5** and triethylamine, in CD_3CN led directly to **6**. Application of a second pulse of CCl_3CO_2H then generated **7** (see Supplementary Information, Section 2.2).

We next demonstrated that it is possible to release the macrocycles from **7** in a stepwise fashion. As the hydrazone and disulfide barriers are labile under orthogonal conditions, we could selectively remove either barrier leaving the other intact. The bulky hydrazone group of **7** was exchanged with the smaller methylhydrazine (Supplementary Information, Section 2.3). The resulting pseudo[3]rotaxane spontaneously dethreaded to the corresponding [2]rotaxane, with the remaining macrocycle still trapped by the disulfide barrier. Reductive cleavage by

addition of dithiothreitol (DTT) then removed the disulfide barrier, dethreading the second macrocycle into the bulk solution (Supplementary Information, Section 2.3). These experiments demonstrated a protocol whereby molecular ratchet **1** could be used to pump from, and then sequentially release the substrate back into, solution.

Finally, we demonstrated the ability of immobilised molecular ratchets to pump substrates from the solution phase to the surface of polymer beads (Fig. 4). A derivative of **1** with a terminal alkyne in place of the 3,5-dimethoxyphenyl stopper was attached to azide-functionalised polystyrene beads by conventional copper-catalysed azide-alkyne cycloaddition (CuAAC) click chemistry.[57] The formation of solid-phase pump **10** was monitored by Fourier-transform Infrared (FTIR) spectroscopy, using the decrease in the intensity of the azide band absorption peak at 2090 cm^{-1} (see Supplementary Information, Section 6). For beads with a diameter of 10 μm, ~8×10^{10} molecular pumps are attached at the solvent-accessible surface of each bead, assuming a penetration depth of 0.5 μm.[39]

To analyse the operation of the immobilised molecular pump, and to demonstrate that the bound substrate is isolated within discrete compartments, we employed crown ethers labelled with anthracene (**8**; fluorescent under excitation at 350 nm) or naphthalimide (**9**; fluorescent under excitation at 420 or 470 nm) tags detectable using fluorescence microscopy and spectroscopy (Fig. 2a).

The operation of **10** was carried out in analogous fashion to pump **1** (Fig. 4). The progress of the fuelled uptake if the crown ethers onto the beads was followed by fluorescence microscopy (see Supplementary Information, Section 4.1). Each stage of the pump operation was analysed by washing the beads with CH_2Cl_2 and CH_3CN to remove residual macrocycle, followed by microscopy of a sample of beads on a glass surface (Fig. 4 shows fluorescence microscopy of beads from before and after each operation to illustrate the change in appearance of the beads after pumping). Initially the beads, **10**, displayed only weak fluorescence when excited at either 350 nm or 470 nm (Fig. 4b and 4c). No increase or change in fluorescence occurred after the beads were suspended in CH_3CN with either **8** or **9**, alongside **2**, **4** or **5**. However, 18 h after a single pulse of CCl_3CO_2H to beads of **10** in a 2.8 mM acetonitrile solution of **8**, afforded **11** (the initial acidity promoting threading, followed by decarboxylation and the regeneration of the basic pH over 18 h), which displayed a four-fold increase in fluorescence intensity when excited with 350 nm UV light, indicative of the presence of **8** on the beads (Fig. 4b). Exhaustive washing of the beads did not decrease the fluorescence intensity, illustrating that **8** is, indeed, mechanically locked onto the axles of the molecular pumps immobilised on **11**. Subjecting beads **11** to a second pulse of CCl_3CO_2H, this time in a 2.8 mM acetonitrile solution of **9**, afforded **12**. The successful pumping of **9** onto the beads was evidenced by a six-fold increase in fluorescence intensity (compared to **10** or **11**) upon excitation at 470 nm (Fig. 4b).

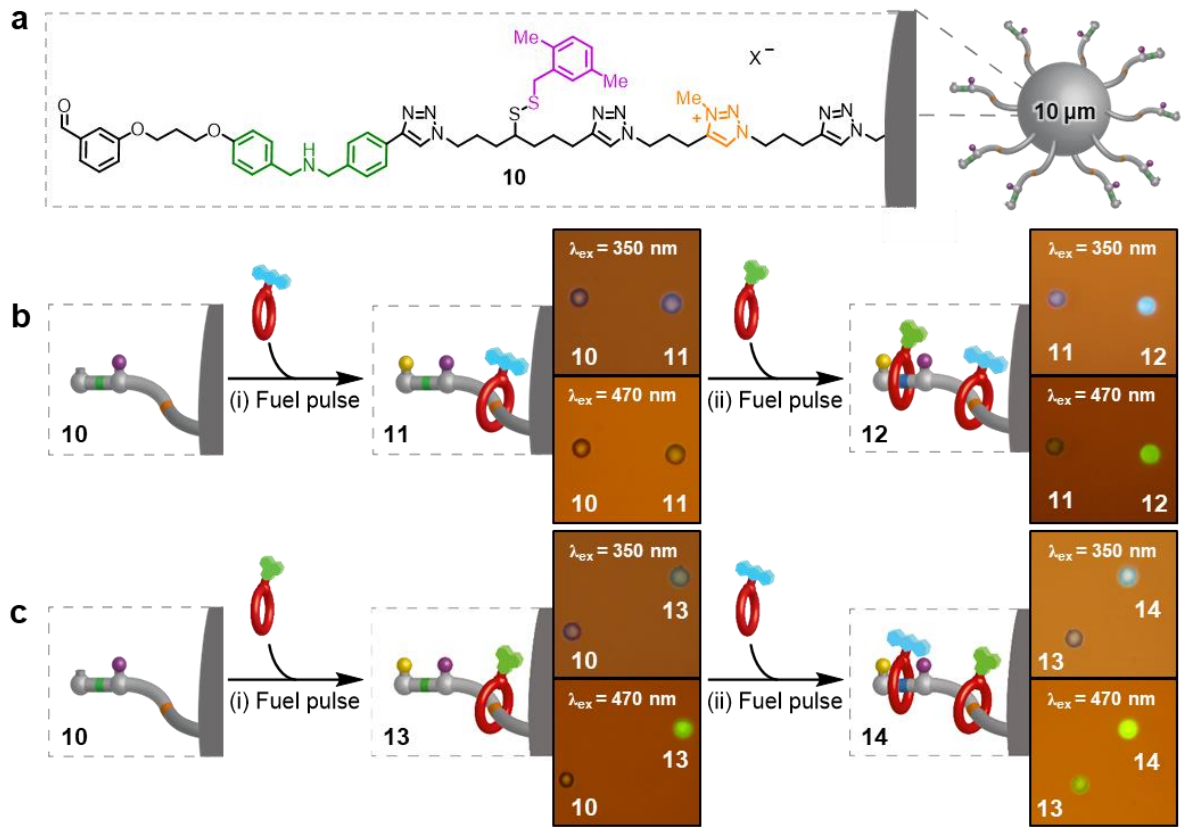

Fig. 4 | Sequential pumping from solution onto polymer beads with a pulsed chemical fuel. **a**, Structure of molecular ratchet immobilised on 10 μm diameter polystyrene beads crosslinked with 1% divinylbenzene (DVB) **10**. **b**, Operation conditions: (i) Beads **10** (0.5 mmol), anthracene macrocycle **8** (2.8 mM), hydrazide **2** (1.1 mM), thiol **5** (1.3 mM), disulfide **6** (13 mM), Et_3N (400 mM) then CCl_3CO_2H (1200 mM), CH_3CN, r.t., 18 h. (ii) Beads **11** (0.5 mmol), naphthalimide macrocycle **9** (2.8 mM), hydrazide **2** (1.1 mM), thiol **5** (1.3 mM), disulfide **6** (13 mM), Et_3N (400 mM) then CCl_3CO_2H (1200 mM), CH_3CN, r.t., 18 h. **c**, Operation conditions: (i) Beads **10** (0.5 mmol), naphthalimide macrocycle **9** (2.8 mM), hydrazide **2** (1.1 mM), thiol **5** (1.3 mM), disulfide **6** (13 mM), Et_3N (400 mM) then CCl_3CO_2H (1200 mM), CH_3CN, r.t., 18 h. (ii) Beads **13** (0.5 mmol), anthracene macrocycle **8** (2.8 mM), hydrazide **2** (1.1 mM), thiol **5** (1.3 mM), disulfide **6** (13 mM), Et_3N (400 mM) then CCl_3CO_2H (1200 mM), CH_3CN, r.t., 18 h. X^- denotes different anions that change during the operation. Fluorescence microscopy images comparing reacted polymer beads, excited with either 350 or 470 nm light, alongside a similar bead prior to reaction (**10**, **11** or **13**).

Crown ethers **8** and **9** could also be pumped onto the beads to form a different sequence isomer[40] on the molecular axles (Fig. 4c). Reversing the order of macrocycle pumping gave bead **13**, which exhibited a six-fold increase in fluorescence intensity when excited with 470 nm light, and then bead **14**, which had a two-fold increase in fluorescence intensity when excited with 350 nm light (Fig. 4c).

Beads of **12** and **14**, which differ only in the sequence of the rings on the axle,[40] are effectively indistinguishable by fluorescence microscopy at all wavelengths (Fig. 4b cf. 4c). However, the sequence information stored in the beads by ratcheting to their out-of-equilibrium states can be revealed by successive release of the macrocycles from the different compartments of the

axle (Fig. 5). Treatment of rotaxane-bead **12** with methylhydrazine followed by Et_3N in acetonitrile, gave a supernatant solution which was analysed by fluorescence spectroscopy. Upon excitation at 420 nm (the wavelength of maximum absorption of the tag but unavailable with our fluorescence microscopy set up), the fluorescence emission centred at 520 nm is characteristic of macrocycle **9** (left hand spectrum, Fig. 5a). The resulting bead **15** was then treated with dithiothreitol (DTT; to cleave the disulfide barrier) liberating **8** into solution, as indicated by the characteristic fluorescence emission at 395 nm when excited with 350 nm UV light (right hand spectrum, Fig. 5a). Subjecting the sequence isomer rotaxane-bead **14** to the same cleavage protocols, the order of macrocycle release was reversed (Fig 5b).

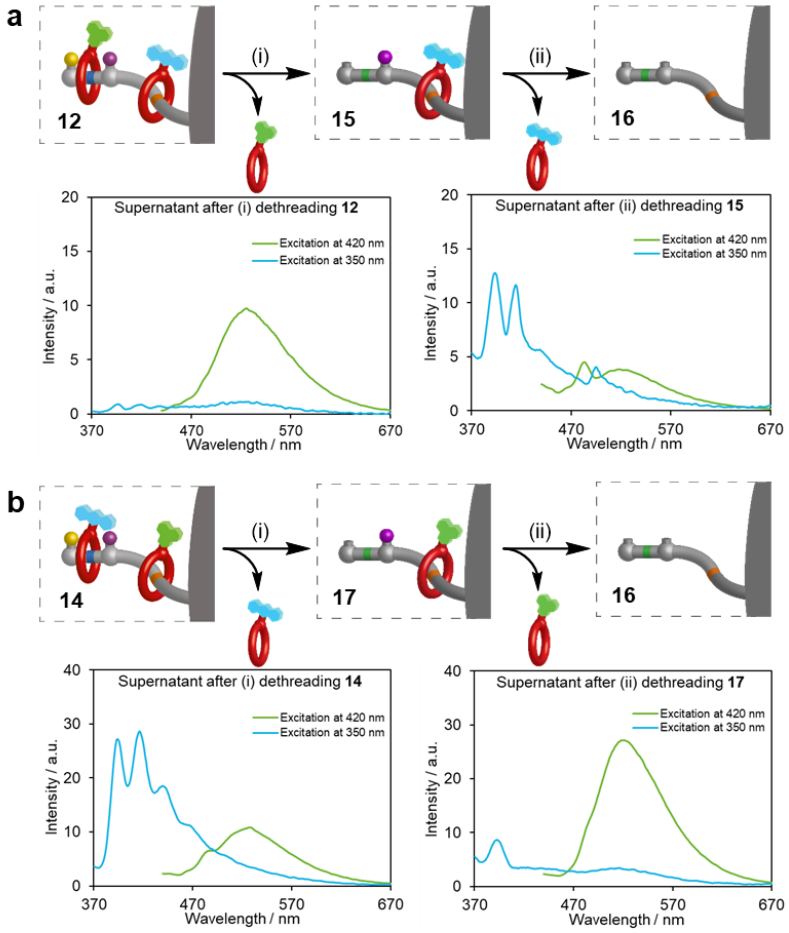

Fig. 5 | Reading of sequence information stored in ratcheted rotaxane polymer beads. **a**, Operation conditions: (i) Beads **12** (0.5 mmol), methylhydrazine (200 mM), CF_3CO_2H (50 mM), CH_3CN, r.t., 24 h. (ii) Beads **15** (0.5 mmol), DTT (50 mM), Et_3N (50 mM), CH_3CN, r.t., 24 h. **b**, Operation conditions: (i) Beads **14** (0.5 mmol), methylhydrazine (200 mM), CF_3CO_2H (50 mM), CH_3CN, r.t., 24 h. (ii) Beads **17** (0.5 mmol), DTT (50 mM), Et_3N (50 mM), CH_3CN, r.t., 24 h. Fluorescence emission spectra of the corresponding supernatant acetonitrile solutions after dethreading were measured by excitation at 350 nm (blue) to detect the presence of anthracene tag **8** and 420 nm (green) to detect the presence of naphthalimide tag **9**.

The energy input for life largely originates from light (via photosynthesis). However, biology uses chemical fuels[58] as the primary mediators of energy to power[59] the complex nonequilibrium nanotechnology of the cell. Here we have demonstrated that immobilised

molecular ratchets can transduce energy from a chemical fuel for the non-equilibrium transport of substrates from one phase of matter to another. Such processes may prove useful for the extraction of chemicals from solution (or the gas phase) and the storage and release of both energy and information, by and for artificial molecular nanotechnology.[60]

Methods

Methods, including statements of data availability, are available at http://doi.org/xxxxxxxxx

References

1. Zhuang, J., Gordon, M. R., Ventura, J., Li, L. & Thayumanavan, S. Multi-stimuli responsive macromolecules and their assemblies. *Chem. Soc. Rev.* **42**, 7421–7435 (2013).

2. Yang, Y.-W., Sun, Y.-L. & Song, N. Switchable host–guest systems on surfaces. *Acc. Chem. Res.* **47**, 1950–1960 (2014).

3. Kolesnichenko, I. V. & Anslyn, E. V. Practical applications of supramolecular chemistry. *Chem. Soc. Rev*. **46**, 2385–2390 (2017).

4. Kay, E. R., Leigh, D. A. & Zerbetto, F. Synthetic molecular motors and mechanical machines. *Angew. Chem. Int. Ed.* **46**, 72–191 (2007).

5. Pezzato, C., Cheng, C., Stoddart, J. F. & Astumian, R. D. Mastering the non-equilibrium assembly and operation of molecular machines. *Chem. Soc. Rev.* **46**, 5491–5507 (2017).

6. Zhang, L., Marcos, V. & Leigh, D. A. Molecular machines with bio-inspired mechanisms. *Proc. Natl. Acad. Sci. USA* **115**, 9397–9404 (2018).

7. Astumian, R. D. et al. Non-equilibrium kinetics and trajectory thermodynamics of synthetic molecular pumps. *Mater. Chem. Front.* **4**, 1304–1314 (2020).

8. Astumian, R. D. Irrelevance of the power stroke for the directionality, stopping force, and optimal efficiency of chemically driven molecular machines. *Biophys. J.* **108**, 291–303 (2015).

9. Erbas-Cakmak, S., Leigh, D. A., McTernan, C. T. & Nussbaumer, A. L. Artificial molecular machines. *Chem. Rev.* **115**, 10081–10206 (2015).

10. Astumian, R. D., Mukherjee, S. & Warshel, A. The physics and physical chemistry of molecular machines. *ChemPhysChem* **17**, 1719–1741 (2016).

11. Amano, S., Fielden, S. D. P. & Leigh, D. A. A catalysis-driven artificial molecular pump. *Nature* **594**, 529–534 (2021).

12. Borsley, S., Leigh, D. A. & Roberts, B. M. W. A doubly kinetically-gated information ratchet autonomously driven by carbodiimide hydration. *J. Am. Chem. Soc*. **143**, 4414–4420 (2021).

13. Boekhoven, J., Hendriksen, W. E., Koper, G. J. M., Eelkema, R. & van Esch, J. H. Transient assembly of active materials fueled by a chemical reaction. *Science* **349**, 1075–1079 (2015).

14. De, S. & Klajn, R. Dissipative self-assembly driven by the consumption of chemical fuels. *Adv. Mater.* **30**, 1706750 (2018).

15. van Rossum, S. A. P., Tena-Solsona, M., van Esch, J. H., Eelkema, R. & Boekhoven, J. Dissipative out-of-equilibrium assembly of man-made supramolecular materials. *Chem. Soc. Rev.* **46**, 5519−5535 (2017).

16. Ragazzon, G. & Prins, L. J. Energy consumption in chemical fuel-driven self-assembly. *Nat. Nanotechnol.* **13**, 882−889 (2018).

17. Serreli, V., Lee, C.-F., Kay, E. R. & Leigh, D. A. A molecular information ratchet. *Nature* **445**, 523–527 (2007).

18. Ragazzon, G., Baroncini, M., Silvi, S., Venturi, M. & Credi, A. Light-powered autonomous and directional molecular motion of a dissipative self-assembling system. *Nat. Nanotechnol.* **10**, 70–75 (2015).

19. Cheng, C. et al. An artificial molecular pump. *Nat. Nanotechnol.* **10**, 547–553 (2015).

20. Erbas-Cakmak, S. et al. Rotary and linear molecular motors driven by pulses of a chemical fuel. *Science* **358**, 340–343. (2017).

21. Pezzato, C. et al. Controlling dual molecular pumps electrochemically. *Angew. Chem. Int. Ed.* **57**, 9325–9329 (2018).

22. Qiu, Y. et al. A precise polyrotaxane synthesizer. *Science* **368**, 1247–1253 (2020).

23. Qiu, Y., Feng, Y., Guo, Q.-H., Astumian, R. D. & Stoddart, J. F. Pumps through the ages. *Chem* **6**, 1952–1977 (2020).

24. Balzani, V., Credi, A. & Venturi, M. Molecular machines working on surfaces and at interfaces. *ChemPhysChem* **9**, 202–220 (2008).

25. Davis, J. J., Orlowski, G. A., Rahman, H. & Beer, P. D. Mechanically interlocked and switchable molecules at surfaces. *Chem. Commun.* **46**, 54–63 (2010).

26. Zhang, Q. & Qu, D.-H. Artificial molecular machine immobilized surfaces: A new platform to construct functional materials. *ChemPhysChem* **17**, 1759–1768 (2016).

27. R. D. Astumian, I. Derényi, Fluctuation driven transport and models of molecular motors and pumps. *Eur. Biophys. J.* **27**, 474–489 (1998).

28. Hernández, J. V., Kay, E. R. & Leigh, D. A. A reversible synthetic rotary molecular motor. *Science* **306**, 1532–1537 (2004).

29. Chatterjee, M. N., Kay, E. R. & Leigh, D. A. Beyond switches: Ratcheting a particle energetically uphill with a compartmentalized molecular machine. *J. Am. Chem. Soc*. **128**, 4058–4073 (2006).

30. Barrell, M. J., Campaña, A. G., von Delius, M., Geertsema, E. M. & Leigh, D. A. Light-driven transport of a molecular walker in either direction along a molecular track. *Angew. Chem. Int. Ed*. **50**, 285–290 (2011).

31. Kassem, S., Lee, A. T. L., Leigh, D. A., Markevicius, A. & Solà, J. Pick-up, transport and release of a molecular cargo using a small-molecule robotic arm. *Nat. Chem.* **8**, 138–143 (2016).

32. Berrocal, J. A., Biagini, C., Mandolini, L. & Di Stefano, S. Coupling of the decarboxylation of 2-cyano-2-phenylpropanoic acid to large-amplitude motions: a convenient fuel for an acid-base-operated molecular switch. *Angew. Chem. Int. Ed.* **55**, 6997–7001 (2016).

33. Ghosh, A., Paul, I., Adlung, M., Wickleder, C. & Schmittel, M. Oscillating emission of [2]rotaxane driven by chemical fuel. *Org. Lett*. **20**, 1046–1049 (2018).

34. Shiab, Q. & Chen, C.-F. Step-by-step reaction-powered mechanical motion triggered by a chemical fuel pulse. *Chem. Sci*. **10**, 2529–2533 (2019).

35. Biagini, C., Fielden, S. D. P., Leigh, D. A., Schaufelberger, F., Di Stefano, S. & Thomas, D. Dissipative catalysis with a molecular machine. *Angew. Chem. Int. Ed*. **58**, 9876–9880 (2019).

36. Biagini, C. & Di Stefano, S. Abiotic chemical fuels for the operation of molecular machines. *Angew. Chem. Int. Ed.* **59**, 8344–8354 (2020).

37. Olivieri, E., Quintard, G., Naubron, J.-V. & Quintard, A. Chemically fueled three-state chiroptical switching supramolecular gel with temporal control. *J. Am. Chem. Soc*. **143**, 12650–12657 (2021).

38. Abe, Y., Okamura, H., Nakazono, K., Koyama, Y., Uchida, S. & Takata, T. Thermoresponsive shuttling of rotaxane containing trichloroacetate ion. *Org. Lett*. **14**, 4122–4125 (2012).

39. Asthana, D. et al. Studies of inorganic-organic [10^{14}]rotaxanes: particle-by-particle EPR study and spin counting of micrometre-sized beads decorated with TEMPO-functionalised {Cr_7Ni} heterometallic wheels. submitted for publication.

40. Fuller, A.-M. L., Leigh, D. A. & Lusby, P. J. Sequence isomerism in [3]rotaxanes. *J. Am. Chem. Soc.* **132**, 4954–4959 (2010).

41. Li, Z., Barnes, J. C., Bosoy, A., Stoddart, J. F. & Zink, J. I. Mesoporous silica nanoparticles in biomedical applications. *Chem. Soc. Rev.* **41**, 2590–2605 (2012).

42. Tan, L.-L. *et al.*, Stimuli-responsive metal–organic frameworks gated by pillar[5]arene supramolecular switches. *Chem. Sci.* **6**, 1640–1644 (2015).

43. Meng, X., Gui, B., Yuan, D., Zeller, M. & Wang, C. Mechanized azobenzene-functionalized zirconium metal-organic framework for on-command cargo release. *Sci. Adv.* **2**, e1600480 (2016).

44. van Esch, J. H., Klajn, R. & Otto, S. Chemical systems out of equilibrium. *Chem. Soc. Rev.* **46**, 5474–5475 (2017).

45. Berná, J., Leigh, D. A., Lubomska, M., Mendoza, S. M., Pérez, E. M., Rudolf, P., Teobaldi, G. & Zerbetto, F. Macroscopic transport by synthetic molecular machines. *Nat. Mater*. **4**, 704–710 (2005).

46.Vukotic, V. N., Harris, K. J., Zhu, K. L., Schurko, R. W. & Loeb, S. J. Metal-organic frameworks with dynamic interlocked components. *Nat. Chem.* **4**, 456–460 (2012).

47. Zhu, K. L., O'Keefe, C. A., Vukotic, V. N., Schurko, R. W. & Loeb, S. J. A molecular shuttle that operates inside a metal-organic framework. *Nat. Chem.* **7**, 514–519 (2015).

48. Watson, M. A. & Cockroft, S. L. Man-made molecular machines: membrane bound. *Chem. Soc. Rev.* **45**, 6118–6129 (2016).

49. Martinez-Bulit, P., Stirk, A. J. & Loeb, S. J. Rotors, motors, and machines inside metal-organic frameworks. *Trends Chem.* **1**, 588–600 (2019).

50. Danowski, W. *et al.*, Unidirectional rotary motion in a metal-organic framework. *Nat. Nanotechnol.* **14**, 488–494 (2019).

51. Krause, S. & Feringa, B. L. Towards artificial molecular factories from framework-embedded molecular machines. *Nat. Rev. Chem.* **4**, 550–562 (2020).

52. Mena-Hernando, S. & Pérez, E. M. Mechanically interlocked materials. Rotaxanes and catenanes beyond the small molecule. *Chem. Soc. Rev.* **48**, 5016–5032 (2019).

53. Aprahamian, I. The future of molecular machines. *ACS Cent. Sci.* **6**, 347–358 (2020).

54. Heard, A. W. & Goldup, S. M. Simplicity in the design, operation, and applications of mechanically interlocked molecular machines. *ACS Cent. Sci*. **6**, 117–128 (2020).

55. Wilson, M. R., Solá, J., Carlone, A., Goldup, S. M., Lebrasseur, N. & Leigh, D. A. An autonomous chemically fuelled small-molecule motor. *Nature* **534**, 235–240 (2016).

56. Coutrot, F. A focus on triazolium as a multipurpose molecular station for pH-sensitive interlocked crown-ether-based molecular machines. *ChemistryOpen* **4**, 556–576 (2015).

57. Liang, L. & Astruc, D. The copper(I)-catalyzed alkyne-azide cycloaddition (CuAAC) “click” reaction and its applications. An overview. *Coord. Chem. Rev*. **255**, 2933–2945 (2011).

58. Walsh, C. T., Tu, B. P. & Tang, Y. Eight kinetically stable but thermodynamically activated molecules that power cell metabolism. *Chem. Rev.* **118**, 1460–1494 (2018).

59. Amano, S., Borsley, S., Leigh, D. A. & Sun, Z. Chemical engines: Driving systems away from equilibrium through catalyst reaction cycles. *Nat. Nanotechnol*. **16**, 1057–1067 (2021).

60. We have deposited this manuscript on ChemRxiv, whilst it is undergoing journal peer review, to coincide with the publication of a related paper from the Stoddart group that describes the out-of-equilibrium adsorption of rings into MOFs by electrochemically driven molecular pumps, a process that the authors term ‘mechanisorption’. We are grateful to Sir Fraser for its advanced disclosure.

Acknowledgements

The authors thank Prof S. Webb and D. Heyes for assistance with the fluorescence microscopy and spectroscopy, Dr S. D. P. Fielden for useful discussions, the University of Manchester Mass Spectrometry Service Centre for high-resolution mass spectrometry, the

Engineering and Physical Sciences Research Council (EPSRC; EP/P027067/1) and the EU (European Research Council (ERC); Advanced Grant no. 786630) for funding, and the University of Manchester for a President's Scholarship (to D.T.). D.A.L. is a Royal Society Research Professor.

Author contributions

D.T., D.J.T., Y.R., S.K. and U.K. planned and carried out the experimental work and characterisation studies. D.A.L. directed the research. All authors contributed to the analysis of the results and the writing of the manuscript.

Competing interests

The authors declare no competing interests.

Additional information

Supplementary information is available for this paper at https://doi.org/